Coaxial Fiber Supercapacitor Using All-Carbon Material Electrodes

Viet Thong Le,[†,‡] Heetae Kim,[‡] Arunabha Ghosh,[†,§] Jaesu Kim,[†,‡] Jian Chang,[†,‡] Quoc An Vu,[†,‡] Duy Tho Pham,[†,‡] Ju-Hyuck Lee,[§] Sang-Woo Kim,[†,§] and Young Hee Lee[†,‡,*]

[†]IBS Center for Integrated Nanostructure Physics, Institute for Basic Science (IBS), Daejon 305-701, Republic of Korea, [‡]Department of Energy Science, Department of Physics, Sungkyunkwan University, Suwon 440-746, Republic of Korea, and [§]Sungkyunkwan Advanced Institute of Nanotechnology, School of Advanced Materials Science and Engineering, Sungkyunkwan University, Suwon 440-746, Republic of Korea

ABSTRACT We report a coaxial fiber supercapacitor, which consists of carbon microfiber bundles coated with multiwalled carbon nanotubes as a core electrode and carbon nanofiber paper as an outer electrode. The ratio of electrode volumes was determined by a half-cell test of each electrode. The capacitance reached 6.3 mF cm^{-1} (86.8 mF cm^{-2}) at a core electrode diameter of 230 μm and the measured energy density was 0.7 μWh cm^{-1} (9.8 μWh cm^{-2}) at a power density of 13.7 μW cm^{-1} (189.4 μW cm^{-2}), which were much higher than the previous reports. The change in the cyclic voltammetry characteristics was negligible at 180° bending, with excellent cycling performance. The high capacitance, high energy density, and power density of the coaxial fiber supercapacitor are attributed to not only high effective surface area due to its coaxial structure and bundle of the core electrode, but also all-carbon materials electrodes which have high conductivity. Our coaxial fiber supercapacitor can promote the development of textile electronics in near future.

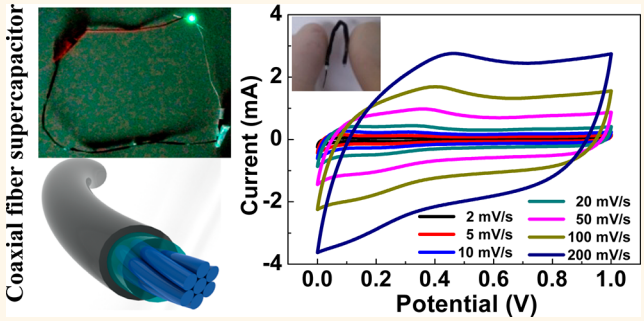

KEYWORDS: supercapacitors · textile electronics · carbon nanotubes · carbon fibers

Fiber electronics, electronic capabilities on textile fibers, is a primary component for wearable technology particularly for future portable and wearable electronics, and is a growing industry.[1−3] Producing electronics components such as transistors,[4−6] and displays,[7] and energy storage and harvesting devices such as solar cells,[8−10] thermoelectric generators,[11] batteries,[12,13] and capacitors[14,15] on fiber electronics is a prerequisite for self-sustaining and self-powered integrated systems. Textile electronics require conducting and/or semiconducting materials to construct electronic capabilities on textile fibers. Metallic fibers have been traditionally used as a core material to load organic transistors and energy converters.[9,16] Although metal fibers have advantages as a core electrode due to their high conductivity and availability, their tendency to oxidize under ambient conditions, poor bendability, and heavy weight limit their uses in wearable electronics.

Not only are carbon microfibers (CMFs) well-known for their high mechanical strength,[17−19] but they are also light, highly conductive, bendable, and inert under ambient conditions, can be woven to form wearable cloths, and are thus attractive as electrode materials for various energy storage devices.[20−27] Most flexible supercapacitors developed thus far have been two-dimensional films using carbon clothes or carbon papers which can be later attached to wearable clothes.[20−28] Even though a supercapacitor is composed of two parallel carbon microfibers,[29] it can be classified as a film type supercapacitor because carbon fibers are placed onto substrate. Recently, cylindrically shaped-fiber supercapacitors have been intensively studied because of their structural advantage for direct use as threads/fabrics in textile electronics.[14,15,30−33] A twisted-fiber supercapacitor was developed using polymer Kevlar fiber covered with ZnO nanorods,[14] but the effective surface area of the structure was low, leading to low capacitance, low energy density, and poor power density, as well as severe leakage current between electrodes during bending. To improve bendability and avoid leakage current,

* Address correspondence to leeyoung@skku.edu.

Received for review April 2, 2013 and accepted June 3, 2013.

Published online June 03, 2013
10.1021/nn4016345

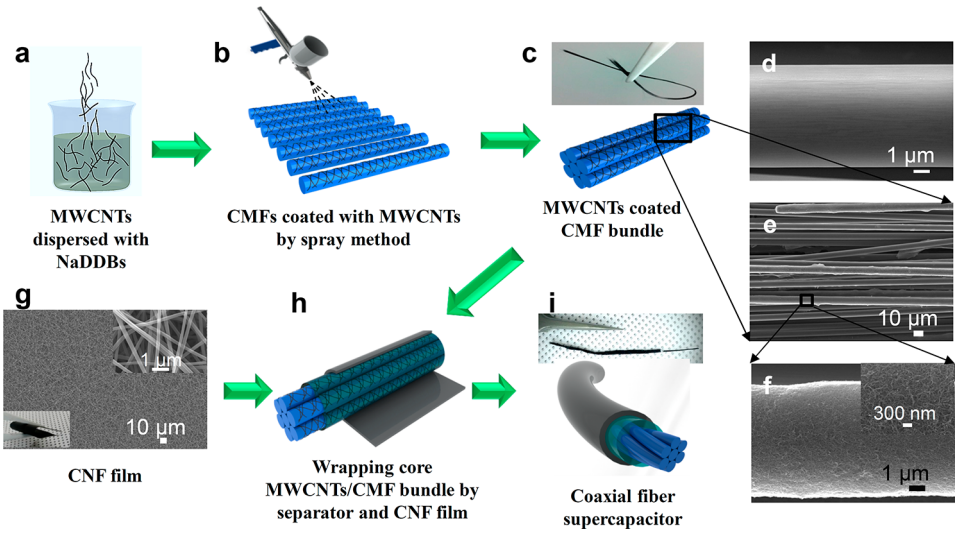

Figure 1. Schematic of the coaxial fiber supercapacitor fabrication process. (a) MWCNTs were dispered in NaDDBs solution. (b) MWCNTs are deposited onto planar CMFs by spray-coating. (c) The MWCNTs/CMFs are assembled into bundles after removing surfactant. (d and f) SEM images of single uncoated CMF and single CMF coated with MWCNTs. (e) SEM image of a MWCNTs/CMF bundle. (g) SEM image of a CNF film and its enlargement on upper right (the inset is a digital photo of the bendable CNF film). (h) After soaking with polymer electrolyte, the core MWCNTs/CMF bundle was wrapped with separator and CNF film. (i) Schematic and digital photo of a coaxial fiber supercapacitor.

two parallel plastic fibers coated with gold and graphite nanoparticles were used to make a flexible fiber supercapacitor by installing spacer wire to prevent contact.[15] However, this supercapacitor still had low capacitance due to its parallel wire structure, limited number of fibers and low conductivity of plastic wires. In order to increase surface area, carbon nanotube fibers and graphene fibers have been used to make fiber supercapacitors.[30−33] In addition to disadvantages of the twisted structures, the above-mentioned capacitors also suffered from poor quality of fibers, which had lower tensile strength and lower conductivity compared to CMFs.[34,35] The choice of electrode materials[36−39] and structure is a key factor in determining the energy and power density of fiber supercapacitor.

Our aim is using CMFs to design a highly flexible coaxial fiber supercapacitor with high energy density and power density which can ultimately be woven into self-powered wearable electronics. In this report, a coaxial fiber supercapacitor was fabricated using all carbon materials. The structure of the developed supercapacitor consisted of a CMF bundle coated with multiwalled carbon nanotubes (MWCNTs) as a core electrode in the center of the coaxial supercapacitor and a carbon nanofiber (CNF) film prepared by electrospinning as an outer electrode. The fabricated coaxial-cable-type supercapacitor provides an efficient, flexible, wearable energy storage device which shows high capacitance, high energy and power density, and good bendability.

RESULTS AND DISCUSSION

Design of Coaxial Fiber Supercapacitor. The fabrication process of a coaxial-cable-type supercapacitor is shown in Figure 1. A commercially available CMF bundle with an individual fiber diameter of ~7 μm was used as a core electrode due to its high mechanical strength (tensile strength ~2 GPa, Figure S1) and high conductivity (~10^3 S/cm). The specific capacitance of CMF is low (0.25 F g^{-1} at a scan rate of 5 mV s^{-1}) due to its low external surface area. To increase the specific capacitance, MWCNTs were coated onto CMF bundle. MWCNTs were dispersed in a sodium dodecylbenzenesulfonate (NaDDBs) solution. A spray method was adopted to deposit MWCNTs on CMF because dipping method yielded nonhomogeneous deposition and poor mechanical adhesion with limitation of massive loading (Supporting Information Figure S2). To coat CMFs with MWCNTs uniformly, the CMF bundle was first spread out on the paper. This was done easily in solution of DI water and isopropyl alcohol by tweezers. The paper was slowly taken out of the solution to prevent CMF aggregation. The prepared planar CMFs were then heated using a hot plate during spray of MWCNTs. The MWCNT droplets were evaporated to leave MWCNTs only on the CMF surface before the next droplets arrived. This enhanced condensation of MWCNTs on the CMF surface and prevented MWCNT aggregation. After coating with MWCNTs, the MWCNTs/CMF was dipped in HNO_3 to remove NaDDBs and then washed with DI water several times. Up to ~90% of the CMF in the bundle was uniformly coated with MWCNTs, as shown in Figure 1d−f. Electrospun CNF film made of polyacrylonitrile (PAN) polymer was used as an outer electrode. PAN nanofiber film with a typical diameter of 200 nm was stabilized in air and further carbonized under argon, which was different from typical activation under CO_2 ambient.[40] This was necessary to maintain the flexibility of the film even though the surface area of the nanofibers is presumably lower. Figure 1g shows FESEM images of the film, and individual CNFs are

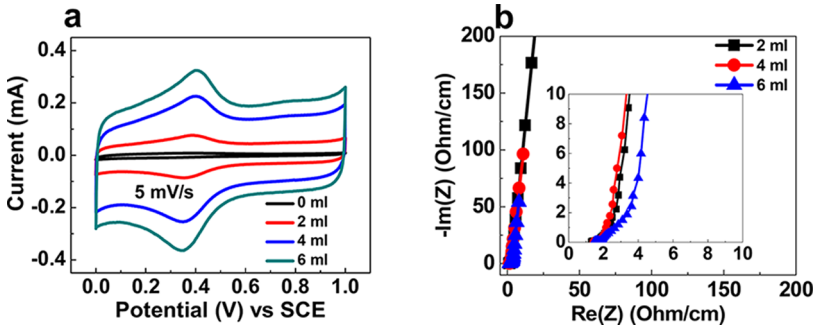

Figure 2. Different volumes of MWCNT solution (2, 4, and 6 mL) loading onto CMF. (a) CV curves at a scan rate of 5 mV s^{-1}. (b) Electrochemical impedance spectroscopy.

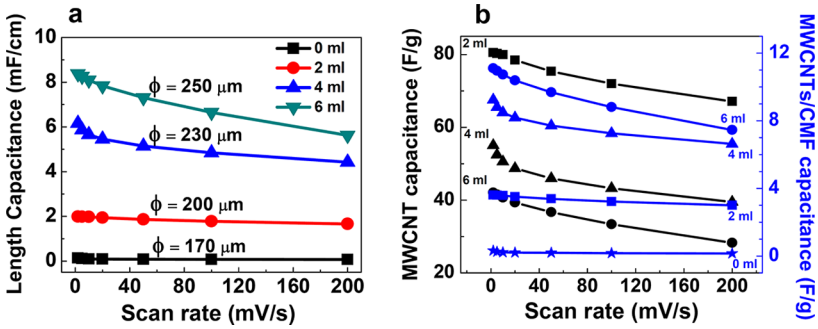

Figure 3. (a) Length capacitance of core electrodes as a function of scan rate with different MWCNT loadings. (b) Gravimetric capacitance of the core electrode calculated for MWCNTs only and for MWCNTs/CMF.

shown in the inset. The bendability of the film is illustrated in the image in the left bottom inset, where the film is shown being bent using tweezers. The core and outer electrode were soaked with polymer electrolyte, and then a separator and the outer electrode were wrapped in series around the core electrode. The final coaxial-cable-type supercapacitor is shown in Figure 1i. Diameter of the final supercapacitor was around 0.8 mm.

Electrochemical Properties of the Core and Outer Electrodes. Figure 2 shows half-cell test with three electrodes of the core electrode with different volumes of MWCNT solution loading. The current was enhanced as the loading content of MWCNTs increased, as shown in Figure 2a. The oxidation peak current reached 0.32 mA at 6 mL, 40 times larger than the 0.0079 mA of pristine CMF. The clear redox peaks are related to electron transfer during redox reaction of hydroxyl and alkoxy groups, as described previously.[41,42] It is intriguing to note that the equivalent series resistance (ESR) was not altered much with the change in MWCNT content, as shown in Figure 2b. The diffusion resistance did not change up to 4 mL MWCNT content, whereas a significant increase in the diffusion resistance was observed at 6 mL MWCNT content. This diffusion resistance originates from the thick MWCNTs accumulated on the CMF surface.

Length capacitance of the core electrode increased as the MWCNT loading was higher, as described in Figure 3a. The diameter of the CMF bundle coated with MWCNTs reached 250 μm at 6 mL from 170 μm of pristine CMF. The length capacitance increased as the MWCNT loading increased due to increased surface area of the MWCNTs/CMF. At larger-diameter MWCNTs/CMF, the capacitance decreased more rapidly as the scan rate increased due to the limited diffusion of ions through the thick MWCNT network. Gravimetric capacitance of MWCNT only or MWCNTs/CMF was shown in Figure 3b. As the MWCNT content increased from 2 to 6 mL, the specific capacitance of MWCNTs decreased from 80 to 42 F g^{-1} due to the limited accessibility of ions in electrolyte, in consistent with the impedance measurements shown in Figure 2b. On the other hand, the specific capacitance of MWCNTs/CMF increased from 3.6 to 11.1 F g^{-1}. The total charge increased as the MWCNT content increased, while the majority of the weight of the sample is due to the CMFs. The decrease in the specific capacitance of the MWCNTs only as the MWCNT loading increased appears similar to the dependence of areal capacitance on SWCNT thickness, as previously reported.[43] For wearable electronics, the fiber diameter is required to be reasonably small, but the fibers must have high capacitance. Hence, we chose 4 mL MWCNT loading, which corresponds to a diameter of 230 μm, to fabricate full-cell coaxial fiber supercapacitors, since the sample with 6 mL loading not only had a large diffusion resistance, leading to poor cycling performance and low power density, but also became rigid and thus had poor flexibility.

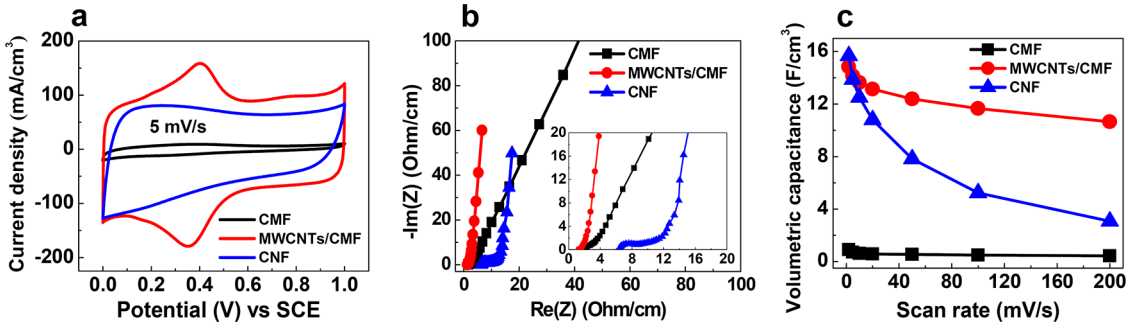

Figure 4. Electrochemical characterizations of a half-cell of CMF, MWCNTs/CMF and CNF. (a) CV curves at a scan rate of 5 mV s^{-1}. (b) Electrochemical impedance spectroscopy. (c) Volumetric capacitance as a function of scan rate.

The electrochemical properties of CNF film as an outer electrode were evaluated and further compared to those of the core electrode as showed in Figure 4. Figure 4a shows cyclic voltammetry (CV) curves measured at a scan rate of 5 mV s^{-1}. The volumetric capacitance of the CMFs without a coating of MWCNTs was 0.7 F cm^{-3}. The volumetric capacitance with MWCNT coating of 4 mL was increased to 14.1 F cm^{-3}, which was 20 times higher than that of CMF only. The high capacitance originates both from pseudocapacitance due to chemical reactions associated with defects and functional groups remaining on the MWCNT surface and from electric double layer capacitance (EDLC).[41,42] The capacitance of the CNFs was 13.8 F cm^{-3}, similar to that of MWCNTs/CMF. The capacitance of the CNFs was mostly attributed to the EDLC. The gravimetric capacitance of the CNF film was 129.8 F g^{-1} at a scan rate of 5 mV s^{-1}, which was 500 times higher than that of CMF and 15 times higher than that of MWCNTs/CMF (Figure S3b). The corresponding electrochemical impedance data is provided in Figure 4b. The ESRs of CMF and MWCNTs/CMF were 1.6 and 1.4 Ω/cm, and revealed that MWCNTs improved the conductivity of the CMF bundle, whereas the ESR of CNF film was 6.8 Ω/cm, much higher than that of MWCNTs/CMF. The slope (tan θ) represents the diffusion of ions in the electrode. Both MWCNTs/CMF and CNF had similar steep slopes, which is different from the tilt slope of the CMF only. Since CMF has a diameter of 7 μm, ultramicropores may be present in the inner area so that ions have difficulty to access which can affect the slope. For the case of MWCNTs/CMF, the CMF surfaces were fully covered by CNTs which block ion diffusion through CMFs. Therefore, ion diffusion through CMFs is prohibited in CMFs and ion diffusion is only limited by the entangled CNTs, which can easily facilitate ion diffusion. On the other hand, the diameter of CNFs is ~200 nm, and micropores are unlikely to be formed during Ar annealing. Therefore, ions can be adsorbed only on the surface, leaving the steep slope, as shown in Figure 4b.

The scan rate dependence on the capacitance was more distinct. While the capacitance of MWCNTs/CMF initially decayed rapidly as the scan rate increased and was saturated at around 50 mV s^{-1}, the capacitance of the CNF decayed over the entire range of scan rate (Figure 4c). Thus, to ensure that our coaxial fiber supercapacitor has good power performance at a high scan rate (or a high current density), we chose a volume ratio between the core and outer electrode by following the ratio of volumetric capacitance C^{V}_{CNF}:$C^{V}_{MWCNTs/CMF}$ = 3:10.6 at scan rate of 200 mV s^{-1}. We fixed the diameter of the MWCNTs/CMF bundle at 230 μm and the length at 5 cm. The volume of the CNF was then controlled by the thickness of the film, which can be adjusted by the volume of PAN precursor used during electrospinning. The thickness of the CNF film at a size of 3.6 cm × 0.4 cm was 40 μm, meaning that the CNF volume was 5.76 mm^3 and the MWCNTs/CMF volume was 1.49 mm^3. Thus, the total capacity balance was C_{CNF}:$C_{MWCNTs/CMF}$ = 17.3:15.8, where the ratio is nearly one.

Electrochemical Performance of Coaxial Fiber Supercapacitors. A coaxial fiber supercapacitor consists of a core and an outer electrode was fabricated following the above ratio. Figure 5a shows the CV curves of the coaxial fiber supercapacitor at various scan rates. The large CV area resembles the EDLC of the outer electrode, whereas a broad oxidation peak was still observed but was slightly upshifted, which resembles the pseudocapacitance of the core electrode. It is worth noting that the redox peaks were retained at high scan rates. This can be attributed to the fact that ion diffusion can be easily facilitated in core electrode with MWCNTs/CMF bundle, because the space between CMFs is quite large (~few micrometers) (Figure 1e), and also high conductivity of CMF promotes electron transfer, in good contrast with film type supercapacitors where the redox peaks are reduced at high scan rate.[44] The ESR of the coaxial fiber supercapacitor was 4.2 Ω/cm (Figure 5b).

As the scan rate varies from 2 to 200 mV s^{-1}, the length capacitance decreased from 6.3 to 2.9 mF cm^{-1}, corresponding to an areal capacitance from 86.8 to 40.4 mF cm^{-2}. The measured capacitance as a function of scan rate is shown in Figure 5c. The capacitance initially dropped, and is saturated at around 50 mV s^{-1}. The theoretical estimated capacitance is shown as a

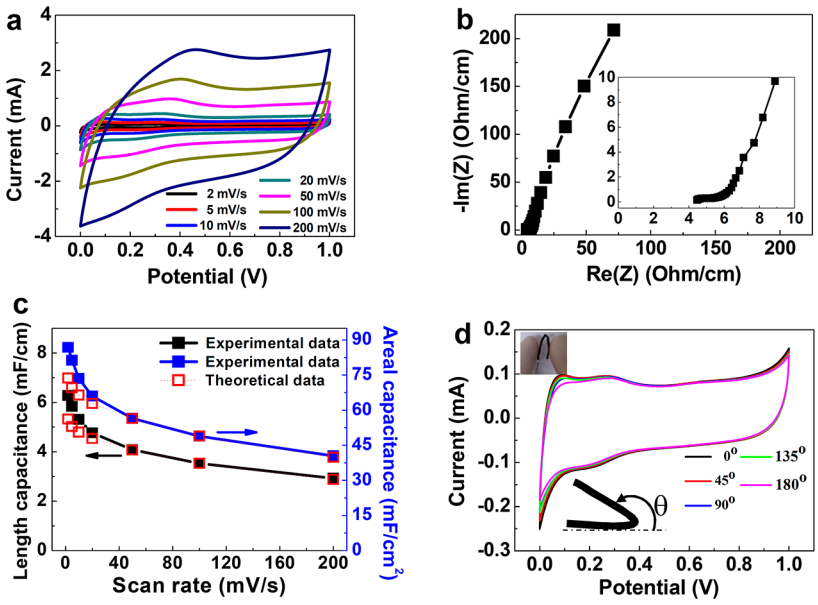

Figure 5. Electrochemical characterizations of the coaxial fiber supercapacitor. (a) CV curves at different scan rates. (b) Electrochemical impedance spectroscopy. (c) Length and areal capacitance from the experimental data and theoretical calculations as a function of scan rate. (d) CV curves with different bending angles at a scan rate of 5 mV s^{-1} (the insets demonstrate the bending angle of the coaxial fiber supercapacitor).

dash line of the equation $(1/C) = [(1/C_c) + (1/C_o)]$, where C_c and C_o are the length capacitance of core and outer electrode, which were determined from the half-cell test. A slight discrepancy was observed at low scan rate. This can be attributed to the fact that the volume of each electrode was optimized by using the values at high scan rate (200 mV s^{-1}). Capacitance depends linearly on length of coaxial fiber supercapacitor as shown in Figure S4. Volumetric capacitance of coaxial fiber capacitor was also calculated by considering the total volume (including volume of two electrodes, electrolyte, and separator), and was supplied in the Supporting Information Figure S5 in order to evaluate its volumetric capacity. Figure 5d shows the CV measurements at a scan rate of 5 mV s^{-1} at different bending angles. The CV shapes were not changed much up to 180° bending, reflecting that the CMF, MWCNTs, and CNF soaked with polymer gel electrolyte are highly flexible. This result implies that our coaxial fiber supercapacitor can be applied for textile flexible electronic devices.

Figure 6a shows typical V-shaped charge−discharge $V-t$ curves at different current densities. The IR drop was small (0.0052 V at 27.5 μA cm^{-1}) benefiting from low ESR. The curves were almost linear, revealing the dominant EDLC contribution. The extracted length capacitance varies from 5.1 to 1.1 mF/cm (corresponding to an areal capacitance of 71.1−14.7 mF/cm^2) in the discharge current density ranges between 0.0275 and 1.375 mA/cm (0.38−19.1 mA/cm^2). Significant reduction of capacitance suggests the slow diffusion of ions at higher discharge currents (Figure 6b). These values are much higher than previous works published recently.[31,32] For instance, two-ply CNT yarn[32] coated with polyaniline showed 12 mF/cm^2 at a current density of 1 mA/cm^2 and two-ply CNT yarn coated with MnO_2[31] showed an areal capacitance of 3.7 mF/cm^2 at very low current of 2 nA. Ragone plot was obtained from the $V-t$ curves shown in Figure 6c. The energy density varied from 0.7 to 0.1 μWh cm^{-1} in a power density range of 13.7−583 μW cm^{-1}. The energy density in terms of the area of the core electrode varied from 9.8 to 1.5 μWh cm^{-2}, corresponding to a power density from 189 to 8070 μW cm^{-2}. This performance is much better than those of a previously reported ZnO-nanowires-coated Kevlar polymer fiber supercapacitor, which showed an energy density of 0.027 μWh cm^{-2} at a power density of 14 μW cm^{-2}[14] or graphite-nanoparticles-coated Ni wire, which showed an energy density range from 2.7 to 1.76 μWh cm^{-2} at a power density range from 42 to 9070 μW cm^{-2}.[15] Compared with these previous works,[14,15,30−33,45] the obtained high capacitance, high energy density and power density in our work can be attributed to three factors: (i) coaxial structure has much more effective area for ion storage compared to twisted structure due to electrolyte existing only at fiber interface,[30−33] (ii) high surface area of MWCNTs-coated CMF bundle compared to single fiber,[14,15,45] and (iii) higher conductivity of CMF bundle. The specific energy density per length of 0.7 μWh cm^{-1} at power density of 13.7 μW cm^{-1}, corresponding to volume energy density of 0.14 mWh cm^{-3} at power density of 2.73 mW cm^{-3}, is slightly better than that of the film supercapacitors in literature[27] and comparable with parallel fiber supercapacitors.[29] In addition, the shape of the coaxial fiber supercapacitor is well-defined and thus the whole size

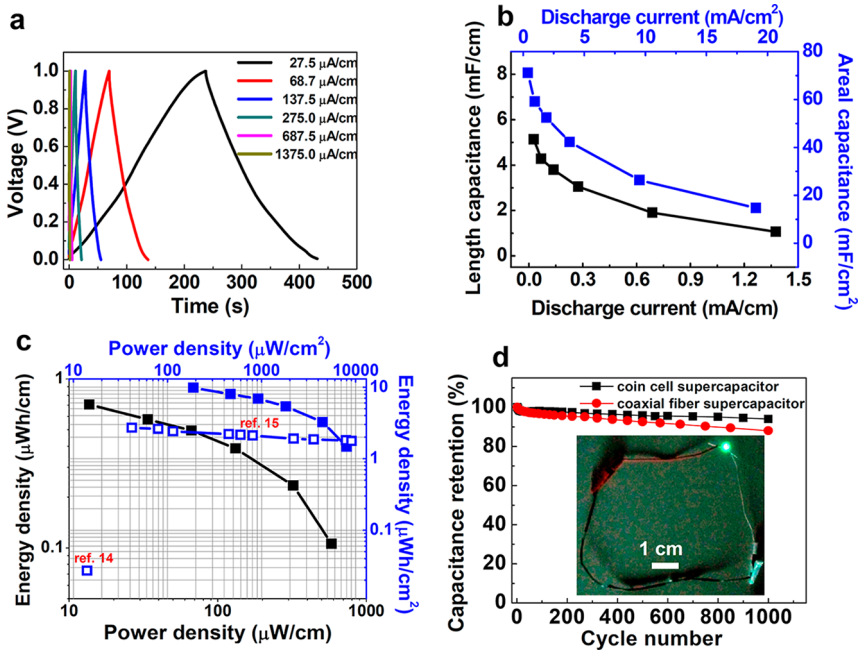

Figure 6. Performance of the coaxial fiber supercapacitor. (a) Charge−discharge curves at different current densities. (b) Length capacitance as a function of current density. (c) Ragone plot with energy and power density per length or area of core-electrode. (d) Cycle performance of coaxial fiber supercapacitor and coin cell supercapacitor at a current density of 275 μA/cm (the inset is LED lighting using four coaxial fiber supercapacitors connected in series, corresponding to 14.4 cm in length).

of the device should be smaller compared to that of parallel structure. Hence, in practice, coaxial structure is preferable. Cycling performance of the coaxial fiber supercapacitor and coin cell supercapacitor at a current density of 275 μA/cm were shown in Figure 6d. Eighty-eight percent of the capacitance of coaxial fiber supercapacitor was retained after 1000 charge−discharge cycles while the coin cell supercapacitor retained 94% capacity of the initial value. The difference in the discharge retention was caused by inefficient sealing in the fiber structure. Finally, to test the feasibility of our coaxial fiber supercapacitor, the four fabricated supercapacitors connected in series with each having a length of 3.6 cm was connected to a green light emitting diode. The inset of Figure 6d shows the green light emitting diode being lit by our coaxial fiber supercapacitor.

Our all-carbon electrodes, CMFs, CNF, and MWCNTs are not only light, but also highly conductive and fully flexible. This is advantageous in comparison to metal wires, which are not flexible upon severe bending, and Kevlar polymer wires which are not conductive. Therefore, our all-carbon materials and coaxial-cable-type supercapacitor is considered to be feasible for use in self-sustainable textile electronics.

CONCLUSION

We have fabricated coaxial fiber supercapacitor using all carbon material electrodes. Our supercapacitor showed good capacitance, high energy density and power density with excellent flexibility. Length capacitance, energy density, and power density are 5.1 mF/cm, 0.7 μWh/cm, and 13.7 μW/cm, respectively. The obtained high capacitance, energy and power density are attributed to high effective surface area of coaxial structure and high conductivity of carbon material, particularly MWCNTs/CMF. Our approach of coaxial fiber supercapacitor will promote the development of textile electronics and self-powered systems in the near future.

METHODS

Preparation of Carbon Nanofiber Film and Carbon Nanotubes Solution. A commercial CMF bundle with an individual fiber diameter of ~7 μm (Jeonju Institute of Machinery and Carbon Composites, Korea) was treated with 12 M HNO_3 for several days. This process is required for the CMFs to be hydrophilic. A CNF film with a fiber diameter of about 200 nm was fabricated using the electrospinning method with PAN diluted in dimethylformamide (DMF) as described previously.[40] The PAN nanofiber film was stabilized in air at 280 °C for 1 h and was carbonized at 800 °C under argon for 1 h.

For preparing the carbon nanotubes solution, MWCNTs with an outer diameter of 10−15 nm (CM 95, Hanwha, Korea) were refluxed in 5 M HNO_3 for 12 h at 120 °C to remove catalysts and then annealed at 500 °C for 2 h to remove amorphous carbon. NaDDBs (purity ~80%, Fluka) of 300 mg was diluted in 100 mL of DI water using a bath sonicator, and 300 mg of the prepared MWCNTs was then added into the NaDDBs solution for dispersion. A high-intensity ultrasonic probe (Ulsso Hitech Co., Korea, Ti-Horn, 19.87 kHz, 700 W) with a power of 60% maximum was used to disperse the CNTs in solution for 60 min. The MWCNT solution was further centrifuged (Hanil Science Industrial Co., Ltd., Mega 17R) at 10 000 rpm for 30 min to remove large bundles and residual catalyst. For preparing gel electrolyte, 10 g of PVA (molecular weight 89 000−98 000, 99+% hydrolyzed,

Aldrich) was diluted into 100 mL of DI water, and 10 g of concentrated H_3PO_4 was then added. This solution was stirred for 3 h at 90 °C to obtain a clear solution.

Fabrication Process of the Coaxial Fiber Supercapacitor. A CMF bundle composed of about 550 fibers with a length of 5 cm was pressed by tweezers to spread the bundle into individual or very small bundles prior to spraying the CNT solution. The spread CMFs were suspended on a hot plate in air. Different volumes of MWCNT solution (2, 4, and 6 mL) were coated on both sides of the CMFs by the spray method. These volumes correspond to CNT weight percents of 4.5, 16.8, and 26.3 wt %. The flattened CMFs coated with MWCNTs were dipped in 5 M HNO_3 for 4 h to remove the surfactant. This again functionalized MWCNTs. The MWCNTs-coated CMF were lightly twisted to form a round bundle for use as the core electrode in a coaxial supercapacitor. The weight of the MWCNTs was measured by the weight difference of the CMF bundle before and after MWCNT deposition. CNF film with a thickness of 40 μm was cut into 3.6 cm $\times$ 0.4 cm pieces. The core electrode and cut CNF film were dipped into gel electrolyte and then transferred into a low vacuum chamber for 0.5 h so that the electrolyte could soak into the pores of the electrodes. After removing from the oven and letting sit for about 20 min, a separator (Celgard 3501, Celgard USA) was rolled around the core electrode and the cut CNF film was rolled on the outside. In this case, the polymer gel electrolyte acted as a glue to attach the outer electrode well.

Characterization. The morphology of the two electrodes was observed by field emission scanning electron microscopy (FESEM, JEOL JSM7000F, Japan), and the capacitive performance of samples was characterized using CV measurement system (Biologic VMP3, France). The electrochemical impedance spectroscopy was measured with a frequency range of 10 kHz to 10 mHz. For the half-cell test, a gold wire was used to connect the core electrode. A custom Teflon cell was used for the coin-type CNF film. A three-electrode configuration was used, with a platinum wire counter electrode and an Ag/AgCl reference electrode, and a MWCNTs-coated CMF bundle or CNF film as the working electrode. For the coaxial fiber supercapacitor test, the two electrodes of the CV system were connected directly to the core and outer electrode of coaxial fiber supercapacitor. To demonstrate the feasibility of the coaxial fiber supercapacitor, a commercial green light emitting diode was used.

Conflict of Interest: The authors declare no competing financial interest.

Acknowledgment. Authors acknowledge Prof. DongSeok Suh for helpful discussion. This work was supported by the Institute for Basic Science (IBS) in Korea and WCU (World Class University) program through the National Research Foundation of Korea funded by the Ministry of Education, Science and Technology (R31-2008-10029). S.-W.K. acknowledges financial support by Basic Science Research Program through the NRF grant funded by the MEST (2010-0015035).

Supporting Information Available: Calculation method; preparation of coin cell; stress−strain curve of CMF; MWCNT loading onto CMF by dipping method; gravimetric capacitance of core and outer electrodes; capacitance as a function of length; volumetric capacitance of coaxial fiber supercapacitor. This material is available free of charge *via* the Internet at http://pubs.acs.org.

REFERENCES AND NOTES

1. Robert, F. S. Electronic Textiles Charge Ahead. *Science* **2003**, *301*, 909–911.
2. Hamedi, M.; Forchheimer, R.; Inganäs, O. Towards Woven Logic from Organic Electronic Fibres. *Nat. Mater.* **2007**, *6*, 357–362.
3. Rossi, D. D. Electronic Textiles: A Logical Step. *Nat. Mater.* **2007**, *6*, 328–329.
4. Hamedi, M.; Herlogsson, L.; Crispin, X.; Marcilla, R.; Berggren, M.; Inganäs, O. Fiber-Embedded Electrolyte-Gated Field-Effect Transistors for E-Textiles. *Adv. Mater.* **2009**, *21*, 573–577.
5. Maccioni, M.; Orgiu, E.; Cosseddu, P.; Locci, S.; Bonfiglio, A. Towards the Textile Transistor: Assembly and Characterization of an Organic Field Effect Transistor with a Cylindrical Geometry. *Appl. Phys. Lett.* **2006**, *89*, 143515.
6. Müller, C.; Hamedi, M.; Karlsson, R.; Jansson, R.; Marcilla, R.; Hedhammar, M.; Inganäs, O. Woven Electrochemical Transistors on Silk Fibers. *Adv. Mater.* **2011**, *23*, 898–901.
7. O'Connor, B.; An, K. H.; Zhao, Y.; Pipe, K. P.; Shtein, M. Fiber Shaped Light Emitting Device. *Adv. Mater.* **2007**, *19*, 3897–3900.
8. Kaltenbrunner, M.; White, M. S.; Głowacki, E. D.; Sekitani, T.; Someya, T.; Sariciftci, N. S.; Bauer, S. Ultrathin and Lightweight Organic Solar Cells with High Flexibility. *Nat. Commun.* **2012**, *3*, 770.
9. Lee, M. R.; Eckert, R. D.; Forberich, K.; Dennler, G.; Brabec, C. J.; Gaudiana, R. A. Solar Power Wires Based on Organic Photovoltaic Materials. *Science* **2009**, *324*, 232–235.
10. O'Connor, B.; Pipe, K. P.; Shtein, M. Fiber Based Organic Photovoltaic Devices. *Appl. Phys. Lett.* **2008**, *92*, 193306.
11. Yadav, A.; Pipe, K. P.; Shtein, M. Fiber-Based Flexible Thermoelectric Power Generator. *J. Power Sources* **2008**, *175*, 909–913.
12. Bhattacharya, R.; Kok, M. M. de; Zhou, J. Rechargeable Electronic Textile Battery. *Appl. Phys. Lett.* **2009**, *95*, 223305.
13. Kwon, Y. H.; Woo, S.-W.; Jung, H.-R.; Yu, H. K.; Kim, K.; Oh, B. H.; Ahn, S.; Lee, S.-Y.; Song, S.-W.; Cho, J.; *et al.* Cable-Type Flexible Lithium Ion Battery Based on Hollow Multi-Helix Electrodes. *Adv. Mater.* **2012**, *24*, 5192–5197.
14. Bae, J.; Song, M. K.; Park, Y. J.; Kim, J. M.; Liu, M.; Wang, Z. L. Fiber Supercapacitors Made of Nanowire-Fiber Hybrid Structures for Wearable/Flexible Energy Storage. *Angew. Chem., Int. Ed.* **2011**, *50*, 1683–1687.
15. Fu, Y.; Cai, X.; Wu, H.; Lv, Z.; Hou, S.; Peng, M.; Yu, X.; Zou, D. Fiber Supercapacitors Utilizing Pen Ink for Flexible/Wearable Energy Storage. *Adv. Mater.* **2012**, *24*, 5713–5718.
16. Nam, S.; Jang, J.; Park, J.-J.; Kim, S. W.; Park, C. E.; Kim, J. M. High-Performance Low-Voltage Organic Field-Effect Transistors Prepared on Electro-Polished Aluminum Wires. *ACS Appl. Mater. Interfaces* **2012**, *4*, 6–10.
17. Chae, H. G.; Kumar, S. Making Strong Fibers. *Science* **2008**, *319*, 908–909.
18. Koziol, K.; Vilatela, J.; Moisala, A.; Motta, M.; Cunniff, P.; Sennett, M.; Windle, A. High-Performance Carbon Nanotube Fiber. *Science* **2007**, *318*, 1892–1895.
19. Khan, U.; Young, K.; O'Neill, A.; Coleman, J. N. High Strength Composite Fibres from Polyester Filled with Nanotubes and Graphene. *J. Mater. Chem.* **2012**, *22*, 12907–12914.
20. Hu, L.; Chen, W.; Xie, X.; Liu, N.; Yang, Y.; Wu, H.; Yao, Y.; Pasta, M.; Alshareef, H. N.; Cui, Y. Symmetrical MnO_2-Carbon Nanotube-Textile Nanostructures for Wearable Pseudocapacitors with High Mass Loading. *ACS Nano* **2011**, *5*, 8904–8913.
21. Yu, G.; Hu, L.; Vosgueritchian, M.; Wang, H.; Xie, X.; McDonough, J. R.; Cui, X.; Cui, Y.; Bao, Z. Solution-Processed Graphene/MnO_2 Nanostructured Textiles for High-Performance Electrochemical Capacitors. *Nano Lett.* **2011**, *11*, 2905–2911.
22. Lu, X.; Wang, G.; Zhai, T.; Yu, M.; Xie, S.; Ling, Y.; Liang, C.; Tong, Y.; Li, Y. Stabilized TiN Nanowire Arrays for High-performance and Flexible Supercapacitors. *Nano Lett.* **2012**, *12*, 5376–5381.
23. Lu, X.; Zhai, T.; Zhang, X.; Shen, Y.; Yuan, L.; Hu, B.; Gong, L.; Chen, J.; Gao, Y.; Zhou, J.; *et al.* WO_{3-x}@Au@MnO_2 Core-Shell Nanowires on Carbon Fabric for High-Performance Flexible Supercapacitors. *Adv. Mater.* **2012**, *24*, 938–944.
24. Cheng, Q.; Tang, J.; Ma, J.; Zhang, H.; Shinya, N.; Qin, L.-C. Polyaniline-Coated Electro-Etched Carbon Fiber Cloth Electrodes for Supercapacitors. *J. Phys . Chem. C* **2011**, *115*, 23584–23590.
25. Hu, L.; Pasta, M.; Mantia, F. L.; Cui, L.; Jeong, S.; Deshazer, H. D.; Choi, J. W.; Han, S. M.; Cui, Y. Stretchable, Porous, and Conductive Energy Textiles. *Nano Lett.* **2010**, *10*, 708–714.
26. Yuan, L.; Lu, X.-H.; Xiao, X.; Zhai, T.; Dai, J.; Zhang, F.; Hu, B.; Wang, X.; Gong, L.; Chen, J.; *et al.* Flexible Solid-State Supercapacitors Based on Carbon Nanoparticles/MnO_2 Nanorods Hybrid Structure. *ACS Nano* **2012**, *6*, 656–661.

27. Yang, P.; Xiao, X.; Li, Y.; Ding, Y.; Qiang, P.; Tan, X.; Mai, W.; Lin, Z.; Wu, W.; Li, T.; *et al.* Hydrogenated ZnO Core-Shell Nanocables for Flexible Supercapacitors and Self-Powered Systems. *ACS Nano* **2013**, *7*, 2617–2626.
28. Yuan, L.; Xiao, X.; Ding, T.; Zhong, J.; Zhang, X.; Shen, Y.; Hu, B.; Huang, Y.; Zhou, J.; Wang, Z. L. Paper-Based Supercapacitors for Self-Powered Nanosystems. *Angew. Chem., Int. Ed.* **2012**, *51*, 4934–4938.
29. Xiao, X.; Li, T.; Yang, P.; Gao, Y.; Jin, H.; Ni, W.; Zhan, W.; Zhang, X.; Cao, Y.; Zhong, J.; *et al.* Fiber-Based All-Solid-State Flexible Supercapacitors for Self-Powered Systems. *ACS Nano* **2012**, *6*, 9200–9206.
30. Chen, T.; Qiu, L.; Yang, Z.; Cai, Z.; Ren, J.; Li, H.; Lin, H.; Sun, X.; Peng, H. An Integrated "Energy Wire" for Both Photoelectric Conversion and Energy Storage. *Angew. Chem., Int. Ed.* **2012**, *51*, 11977–11980.
31. Ren, J.; Li, L.; Chen, C.; Chen, X.; Cai, Z.; Qiu, L.; Wang, Y.; Zhu, X.; Peng, H. Twisting Carbon Nanotube Fibers for Both Wire-Shaped Micro-Supercapacitor and Micro-Battery. *Adv. Mater.* **2013**, *25*, 1155–1159.
32. Wang, K.; Meng, Q.; Zhang, Y.; Wei, Z.; Miao, M. High-Performance Two-Ply Yarn Supercapacitors Based on Carbon Nanotubes and Polyaniline Nanowire Arrays. *Adv. Mater.* **2013**, *25*, 1494–1498.
33. Meng, Y.; Zhao, Y.; Hu, C.; Cheng, H.; Hu, Y.; Zhang, Z.; Shi, G.; Qu, L. All-Graphene Core-Sheath Microfibers for All-Solid-State, Stretchable Fibriform Supercapacitors and Wearable Electronic Textiles. *Adv. Mater.* **2013**, *25*, 2326–2331.
34. Zhang, M.; Atkinson, K. R.; Baughman, R. H. Multifunctional Carbon Nanotube Yarns by Downsizing an Ancient Technology. *Science* **2004**, *306*, 1358–1361.
35. Zhang, X.; Jiang, K.; Feng, C.; Liu, P.; Zhang, L.; Kong, J.; Zhang, T.; Li, Q.; Fan, S. Spinning and Processing Continuous Yarns from 4-Inch Wafer Scale Super-Aligned Carbon Nanotube Arrays. *Adv. Mater.* **2006**, *18*, 1505–1510.
36. Simon, P.; Gogotsi, Y. Materials for Electrochemical Capacitors. *Nat. Mater.* **2008**, *7*, 845–854.
37. Liu, C.; Li, F.; Ma, L.-P.; Cheng, H.-M. Advanced Materials for Energy Storage. *Adv. Mater.* **2010**, *22*, E28–E62.
38. Wang, G.; Zhang, L.; Zhang, J. A Review of Electrode Materials for Electrochemical Supercapacitors. *Chem. Soc. Rev.* **2012**, *41*, 797–828.
39. Ghosh, A.; Lee, Y. H. Carbon-Based Electrochemical Capacitors. *ChemSusChem* **2012**, *5*, 480–499.
40. Ra, E. J.; Raymundo-Piñero, E.; Lee, Y. H.; Béguin, F. High Power Supercapacitors Using Polyacrylonitrile-Based Carbon Nanofiber Paper. *Carbon* **2009**, *47*, 2984–2992.
41. Frackowiak, E.; Metenier, K.; Bertagna, V.; Beguin, F. Supercapacitor Electrodes from Multiwalled Carbon Nanotubes. *Appl. Phys. Lett.* **2000**, *77*, 2421.
42. Pan, H.; Poh, C. K.; Feng, Y. P.; Lin, J. Supercapacitor Electrodes from Tubes-in-Tube Carbon Nanostructures. *Chem. Mater.* **2007**, *19*, 6120–6125.
43. Kaempgen, M.; Chan, C. K.; Ma, J.; Cui, Y.; Gruner, G. Printable Thin Film Supercapacitors Using Single-Walled Carbon Nanotubes. *Nano Lett.* **2009**, *9*, 1872–1876.
44. Zhao, X.; Chu, B. T. T.; Ballesteros, B.; Wang, W.; Johnston, C.; Sykes, J. M.; Grant, P. S. Spray Deposition of Steam Treated and Functionalized Single-Walled and Multi-Walled Carbon Nanotube Films for Supercapacitors. *Nanotechnology* **2009**, *20*, 065605–065613.
45. Bae, J.; Park, Y. J.; Lee, M.; Cha, S. N.; Choi, Y. J.; Lee, C. S.; Kim, J. M.; Wang, Z. L. Single-Fiber-Based Hybridization of Energy Converters and Storage Units Using Graphene as Electrodes. *Adv. Mater.* **2011**, *23*, 3446–3449.